

CPW-Fed Arbitrary Frequency-Switchable Antenna Using CRLH Transmission Line

Inseop Lim and Sungjoon Lim

A novel frequency-switchable antenna that uses PIN diodes and a composite right- and left-handed transmission line (CRLH TL) is proposed. The CRLH TL provides multi-order resonance, including a zeroth-order resonance (ZOR), and its shunt stub determines the ZOR frequency. Thus, the resonant frequency is arbitrarily chosen by lumped chip inductors on the shunt stub. Two prototypes are designed using different chip inductors while maintaining the antenna geometries. Antenna #1 can switch the resonant frequency from 1.8 GHz to 2.3 GHz. Antenna #2 can switch its resonance from 0.9 GHz to 2.3 GHz.

Keywords: Frequency reconfigurable antenna, metamaterial, zeroth-order resonance, ZOR.

I. Introduction

Since mobile communication systems have shown tremendous growth over the past 20 years, it is important to cover multi-frequency bands in a limited space. To cover multi-frequency bands, many researchers have been working on the development of frequency-switchable antennas. Varactor diodes [1], [2] and PIN diodes [3], [4] have been used as the tuning devices. In one study, a tunable low-profile planar inverted-F antenna was presented with a varactor diode [1]. Dual-band tunable slot antennas have also been introduced [2].

Zeroth-order resonance (ZOR) antennas based on a composite right- and left-handed transmission line (CRLH TL) can reduce the antenna size because of its infinite wavelength characteristics and zero phase constant [5]-[7]. When the phase constant is zero, the resonant frequency becomes independent

of the antenna dimensions. In addition to size reduction, vertical polarization can be obtained by a low-profile metamaterial ring antenna [5]. The bandwidth of the ZOR antenna can be increased by co-planar waveguide (CPW) technology [6]. A monopole radiation pattern is obtained with a planar ZOR antenna [5]. Such antennas enable more compactness than conventional half-wavelength antennas. However, in spite of its small size, the ZOR antenna has a narrow bandwidth due to structural problems.

An arbitrary frequency-switchable small antenna using lumped elements and PIN diodes for mobile terminal applications is proposed. The proposed antenna is designed based on a CRLH TL, and its operating frequency is determined by the shunt inductance. Thus, the resonant frequency is switched by the variable inductance, which is realized by two switchable stubs. This switching mechanism becomes possible with a single bias network through an anti-parallel configuration of the PIN diodes at each unit cell.

II. Antenna Design

The proposed CPW antenna, which is designed on a CRLH TL, is able to achieve zeroth-order resonance. A general unit cell model of a CRLH TL consists of a series inductance (L_R), capacitances (C_L and C_R), and a shunt inductance (L_L). It has an infinite wavelength, and its resonant frequency is independent of the size of the resonator. Using these unique properties, the physical size of the antennas can be miniaturized. In the case of an open-ended structure, the resonant frequency of the antenna is determined by the shunt inductance and capacitance.

$$f_r = \frac{1}{2\pi\sqrt{L_L C_R}} \quad (1)$$

Manuscript received Jan. 17, 2013; revised Sept. 6, 2013; accepted Sept. 16, 2013.

This research was supported by the MSIP (Ministry of Science, ICT&Future Planning, Korea, under the ITRC (Information Technology Research Center) support program (NIPA-2013-H0301-13-1002) supervised by the NIPA (National IT Industry Promotion Agency).

Inseop Lim (phone: +82 2 820 5827, topteen85@gmail.com) and Sungjoon Lim (corresponding author, sungjoon@cau.ac.kr) are with the School of Electrical and Electronics Engineering, College of Engineering, Chung-Ang University, Seoul, Rep. of Korea.

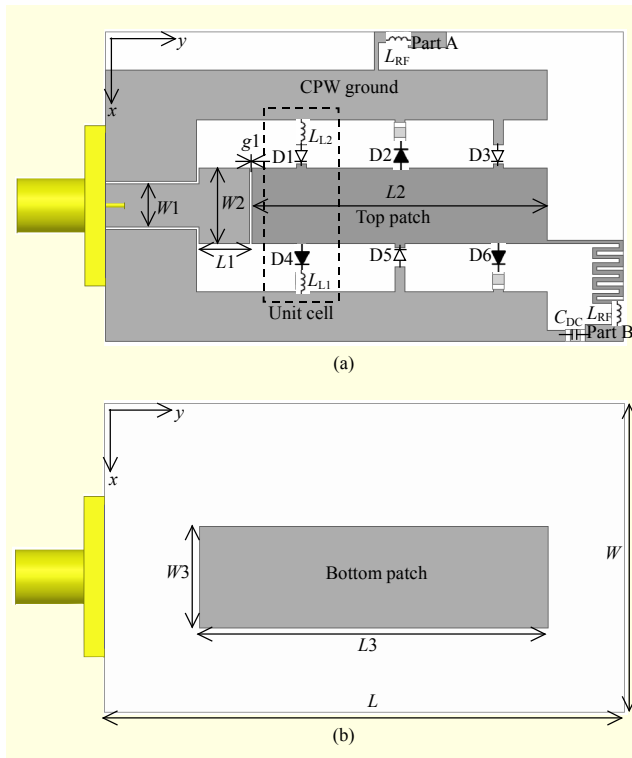


Fig. 1. Geometry of proposed switchable antenna: (a) top view; (b) bottom view.

It is shown that the resonance condition depends on the shunt parameters, and the series components have no effect on the shunt resonance in the proposed antenna. To realize L_L , lumped elements (chip inductors) are connected between the top patch and the CPW grounds, as the shorted stub and the gap between the patch and CPW ground represent C_R . In this study, variable L_L is chosen instead of changing C_R to reconfigure the resonant frequency.

The top and bottom views of the proposed antenna configuration including the bias networks are illustrated in Figs. 1(a) and 1(b), respectively. The antenna consists of a CPW ground, bottom patch, top patch, and feed network. The top patch is composed of three unit cells. To simultaneously supply a voltage to diodes connected on the top patch, three unit cells are cascaded without C_L , which is nonessential for the generation of an infinite wavelength [6]. Since only the shunt components determine the infinite wavelength resonance in the open-ended CRLH TL, it has the same infinite wavelength frequency as a general CRLH TL unit cell. Each unit cell has two shorted stubs. One stub has a single PIN diode and a chip inductor in series, while the other stub has only a single PIN diode. Therefore, the two stubs characterize different inductances (L_{L1} and L_{L2}). L_{L1} comes from the inductance of the chip inductor, while L_{L2} is the inductance of the shorted transmission line. Depending on the voltage supplied on the

PIN diode, one stub is chosen, and the resonant frequency is determined by the inductance of the selected stub. To minimize the number of bias networks, six diodes at each stub are placed in anti-parallel. The voltage at part A is supplied to the CPW ground, and the voltage at part B is supplied to the top patch. When part A is at a high voltage and part B is at a low voltage, diodes D1, D3, and D5 turn on, whereas D2, D4, and D6 are off. Because of the SMA connector, two CPW grounds are connected to each other. Therefore, two CPW grounds have the same potential as part A. On the other hand, when part B is at a high voltage and part A is at a low voltage, diodes D2, D4, and D6 turn on, whereas D1, D3, and D5 are off. Since the current can flow through forward-biased diodes, the shunt inductance can be dramatically changed by controlling the bias voltages at parts A and B. The proposed antenna exhibits multiband resonant behavior. The first resonant frequency is determined by the stubs with a forward-biased diode. In contrast, the second resonant frequency is determined by the stubs mounted on reverse-biased diodes. Even though the diode is reversed, a small current can flow through the reverse-biased diode and influence the second resonant frequency. In Fig. 1(b), the bottom patch is placed under the top patch, which results in a higher coupling capacitance in the feed network for the sake of impedance matching.

III. Fabrication and Results

Figure 2 shows a photograph of the fabricated CPW-fed arbitrary frequency-switchable antenna. It is fabricated on a Rogers RT/Duroid 5880 substrate with a dielectric constant of 2.2 and a thickness of 1.6 mm. The overall area of the antenna is approximately 24.4 mm × 41 mm ($W \times L$). The antenna's dimensional parameters (unit: mm) are $W1=3.4$, $W2=6$, $W3=8$, $L1=4$, $L2=23.4$, $L3=27.5$, and $g1=0.2$, as shown in Figs. 1(a) and 1(b). A CPW feeding line of 50 Ω and proximity coupling are used to provide sufficient impedance matching. For the bias network, a 39-nH chip inductor as an RF choke (L_{RF}) and a 3-pF chip capacitor as a DC block (C_{DC}) are used to isolate between the top patch and the DC bias line. Since the top patch greatly affects the radiation, part B is a quarter wavelength apart from the top patch. The DC bias line is designed to use a meander line, taking into account the overall antenna size. A Skyworks SMP1345-079LF PIN diode is used as the switching element with a forward voltage of $V_F=0.89$ V and a forward-bias current of $I_F=12$ mA. The circuit parameters of the PIN diode with the parasitic packaging effects are obtained from the manufacturer's datasheet. The diode's components are $L_{diode}=0.7$ nH, $C_{diode}=0.18$ pF, and $R_{diode}=2$ Ω . The parasitic resistance, R_p , is higher than the reactance of the capacitance, C_T , and is less significant. These components are considered in

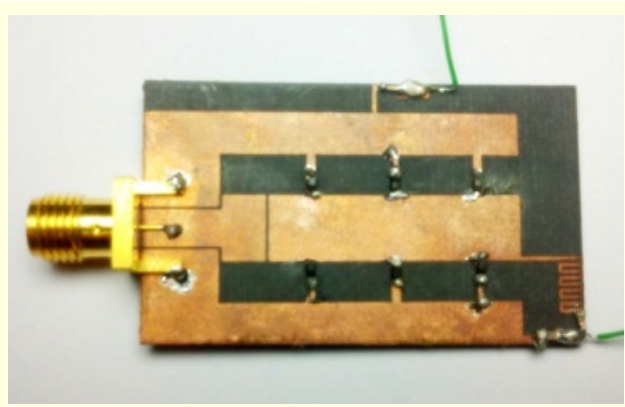


Fig. 2. Fabricated prototype of proposed frequency switchable antenna.

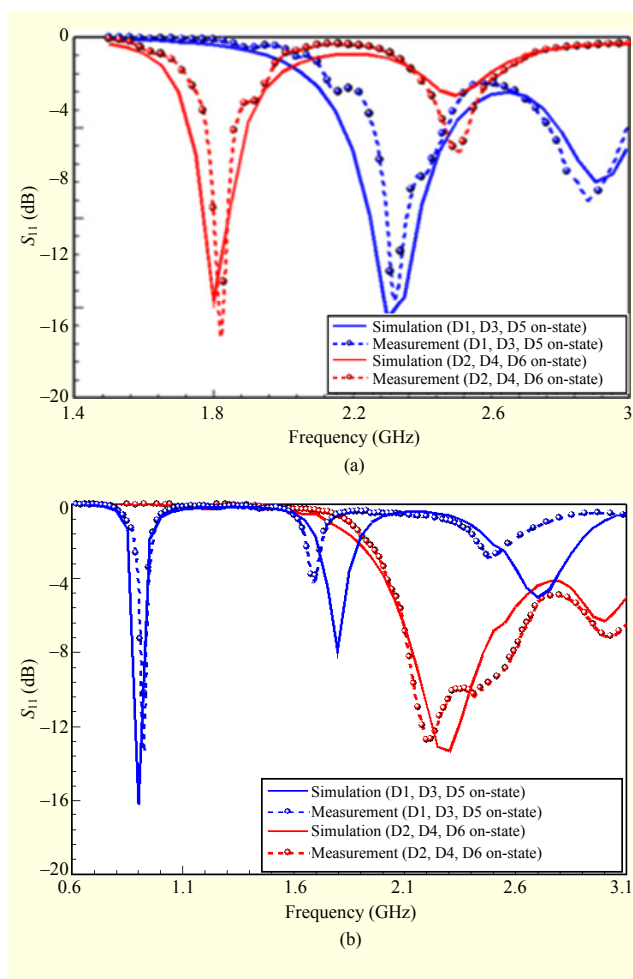


Fig. 3. Measured and simulated reflection coefficient magnitudes of (a) antenna #1 and (b) antenna #2.

all the simulations to fully characterize their effects on the antenna performance. Electromagnetic simulation is performed using ANSYS HFSS.

Two prototypes (antenna #1 and antenna #2) are fabricated

using different chip inductors while maintaining the antenna geometries to demonstrate that the target frequency can be easily changed by lumped chip inductors on the shunt stub. For antenna #1, when part B is supplied with a higher voltage than part A, the shorted stub with 3.58 nH (L_{L1}) is chosen so that the resonant frequency is 1.8 GHz. In contrast, when part A is supplied with a higher voltage than part B, another shorted stub is chosen, so that the resonant frequency is shifted to 2.3 GHz by L_{L2} , which is the equivalent inductance of the shorted transmission line without any chip inductor. Figure 3(a) shows the simulated and measured reflection coefficients for antenna #1. The resonant frequency can be switched by controlling the bias voltage of switches from 1.8 GHz to 2.3 GHz. The measured peak gain of antenna #1 is -2.89 dBi at 1.8 GHz and -2.6 dBi at 2.3 GHz. The efficiency at 1.8 GHz is simulated and measured as 82% and 76.3%, respectively. The efficiency at 2.3 GHz is simulated and measured as 88% and 81.7%, respectively. From antenna theory [8], the gain is increased with higher frequencies. In addition, when the aperture size is decreased, the gain becomes decreased as well. The -2.89 -dBi peak gain at 1.8 GHz is not low compared with other meander line antennas and CRLH ZOR antennas [6], [7].

To increase inductance L_{L2} , the chip inductor is added for antenna #2 without changing the geometry. L_{L2} is the equivalent inductance of the shorted transmission line with the chip inductor. Inductances L_{L1} and L_{L2} in antenna #2 are 3.5 nH and 35 nH with the lumped chip inductor, respectively. When part B is supplied with a higher voltage than part A, the resonant frequency is 2.3 GHz because of another shorted stub with the 3.58-nH chip inductor (L_{L1}). On the other hand, when part A is supplied with a higher voltage than part B, the resonant frequency is 0.9 GHz due to the high inductance of 35 nH (L_{L2}). Finally, the resonant frequency in antenna #2 can be switched from 0.9 GHz to 2.3 GHz, as shown in Fig. 3(b). The measured peak gain of antenna #2 is -4.89 dBi at 0.9 GHz and -0.12 dBi at 2.3 GHz. The simulated and measured efficiency at 0.9 GHz is 80% and 74.8%, respectively. At 2.3 GHz, the simulated and measured efficiency is 87% and 80.3%, respectively. These values are competitive compared with other frequency reconfigurable antennas [3], [4].

Figure 4 shows the simulated and measured radiation patterns of antenna #1. Figures 4(a) and 4(b) show the x-y plane and x-z plane patterns at 1.8 GHz, respectively. In addition, the x-y plane and x-z plane patterns at 2.3 GHz are shown in Figs. 4(c) and 4(d), respectively. Since the selected shorted stubs are different at 1.8 GHz and 2.3 GHz, a slight difference in the radiation patterns is observed in Fig. 4. The cross-polarizations are lower than -12.4 dB. The measured cross-polarization levels are higher than the simulated ones. Figure 5 shows the simulated and measured radiation patterns

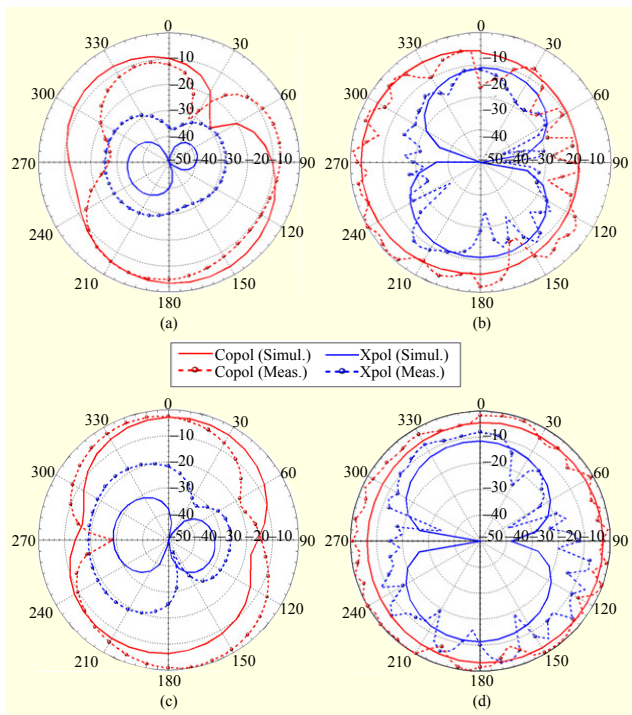


Fig. 4. Measured and simulated radiation patterns of proposed antenna #1: (a) x-y plane at 1.8 GHz, (b) x-z plane at 1.8 GHz, (c) x-y plane at 2.3 GHz, and (d) x-z plane at 2.3 GHz.

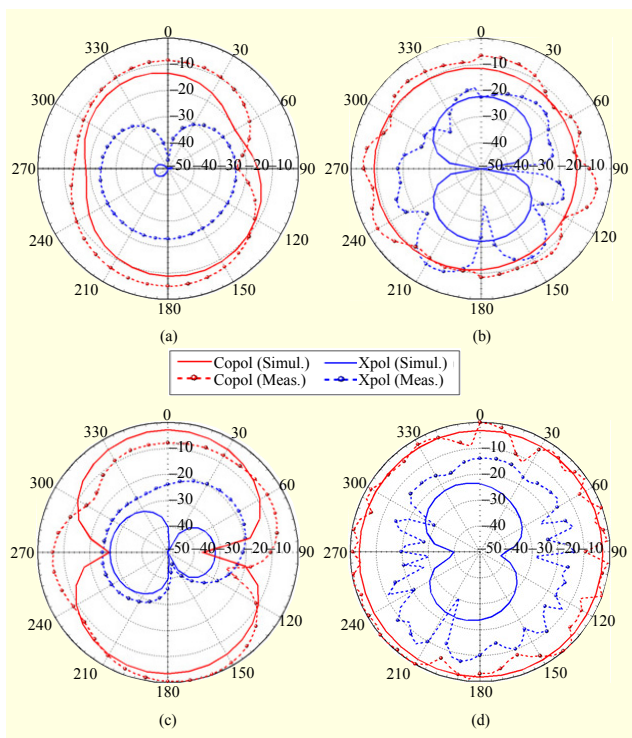


Fig. 5. Measured and simulated radiation patterns of proposed antenna #2: (a) x-y plane at 0.9 GHz, (b) x-z plane at 0.9 GHz, (c) x-y plane at 2.3 GHz, and (d) x-z plane at 2.3 GHz.

of antenna #2. The omnidirectional patterns are necessary for mobile terminal applications.

IV. Conclusion

We proposed a frequency-switchable small antenna. The resonant frequency is successfully switched between 1.8 GHz and 2.3 GHz while maintaining sufficient radiation performances for antenna #1. The switching frequency can be arbitrarily chosen by changing the chip inductors while maintaining the antenna's geometry. Furthermore, for antenna #2, we demonstrated a frequency-switching capability between 0.9 GHz and 2.3 GHz. Therefore, the proposed antenna provides better design feasibility. The proposed switching function can be potentially extended to the arbitrary tri-band switching capability.

References

- [1] P.K. Panayi, M.O. Al-Nuaimi, and L.P. Ivriissimtzis, "Tuning Techniques for Planar Inverted-F Antenna," *Electron. Lett.*, vol. 37, no. 16, Aug. 2001, pp. 1003-1004.
- [2] N. Behdad and K. Sarabandi, "A Varactor-Tuned Dual-Band Slot Antenna," *IEEE Trans. Antennas Propag.*, vol. 54, no. 2, Feb. 2006, pp. 401-408.
- [3] J. Zhong et al., "Quad-band Electrically Small Frequency Reconfigurable Antenna for Handy Terminals," *7th Int. Symp. Wireless Pervasive Comput.*, 2012, pp. 1-3.
- [4] Y.K. Park and Y. Sung, "A Reconfigurable Antenna for Quad-band Mobile Handset Applications," *IEEE Trans. Antenna Propag.*, vol. 60, no. 6, June 2012, pp. 3003-3006.
- [5] A. Lai, T. Itoh, and C. Caloz, "Composite Right/Left-Handed Transmission Line Metamaterials," *IEEE Microw. Mag.*, vol. 5, no. 3, 2004, pp. 34-50.
- [6] T. Jang and S. Lim, "Compact Coplanar Waveguide (CPW)-Fed Zeroth-Order Resonant Antennas with Extended Bandwidth and High Efficiency on Vialess Single Layer," *IEEE Trans. Antennas Propag.*, vol. 59, no. 2, Feb. 2011, pp. 363-372.
- [7] M. Palmdoken, A. Grede, and H. Henke, "Broadband Microstrip Antenna with Left-Handed Metamaterials," *IEEE Trans. Antennas Propag.*, vol. 57, no. 2, Feb. 2009, pp. 331-338.
- [8] R.F. Harrington, "Effect of Antenna Size on Gain, Bandwidth and Efficiency," *J. Research Nat. Bureau Standards-D, Radio Propag.*, vol. 64D, no. 1, 1960, pp. 1-12.